Self-Assembly Growth of Organic Thin Films and Nanostructures by Molecular Beam Deposition. An Interesting and Unexpected Story

Chengzhi Cai,[1,3] Martin Bösch,[1] Christian Bosshard,[1] Bert Müller,[1,3] Ye Tao,[1,3] Armin Kündig,[1] Jens Weckesser,[2] Johannes V. Barth,[2] Lukas Bürgi,[2] Olivier Jeandupeux,[2] Michael Kiy,[1] Ivan Biaggio,[1] Ilias Liakatas,[1] Klaus Kern,[2] and Peter Günter[1]

[1]Nonlinear Optics Laboratory, Institute of Quantum Electronics, Swiss Federal Institute of Technology (ETH), CH-8093 Zurich, Switzerland
[2]Institut de Physique Expérimentale, EPFL, PHB-Ecublens, CH-1015 Lausanne, Switzerland

The concept of supramolecular assemblies based on strong and directional hydrogen bonding has been applied to organic molecular beam deposition (OMBD) for growth of anisotropic nanostructures and thin films. Aligned nanostructures were generated on Ag(111) surfaces. Thin films with a thickness of 100–400 nm were grown on glass substrates by oblique incidence OMBD, and studied by second harmonic generation experiments, indicating that the average direction of the dipolar molecules in the films was parallel to the projection of the molecular beam on the substrate surface. This intriguing result is rationalized by a proposed mechanism considering the fundamental processes of self-assembly on surfaces.

Introduction

Organic thin films and nanostructures have attracted increasing interest for their potential applications in a variety of advanced technologies, including nonlinear optics (NLO), microelectronics, nanotechnology, light emitting devices, field-effect transistors, liquid crystals, sensors, and solar cells (1-7). For many of these applications, the device performance is crucially dependent on the orientation of the functional molecules in the film or the nanostructure (1-3). Therefore, methods for

---

[3]) Current addresses. CC: Department of Chemistry, University of Houston, Houston, TX 77204-5641. BM: Biocompatible Materials Science and Engineering, ETH Zürich. YT: Institute for Microstructural Sciences, National Research Council Canada, M-50 Montreal Road, Rm 178, Ottawa, Ontario, Canada K1A 0R6.

alignment of molecules in the structures are of great technological interest. The alignment can be centrosymmetric or non-centrosymmetric. Non-centrosymmetric alignment is more challenging, because the acentric molecules need to be aligned with a directional preference. It is, however, the basic requirement for organic second order nonlinear optics (1,2) which is our primary interest.

Several techniques have been developed for the growth of anisotropic organic thin films (1-7). For the alignment of molecules perpendicular to the substrate surface, most common techniques include Langmuir-Blodgett (LB) film formation, high electric field poling, and self-assembly using the layer-by-layer methodology (4). For aligning molecules parallel to the substrate surface (in-plane), the anisotropy can be induced by an anisotropic substrate surface (7). However, if an isotropic substrate surface is required, the surface alone cannot induce an in-plane preferential alignment over a large area. To circumvent this problem, external physical means may be applied to impose a preference to the alignment. For example, we have demonstrated that, during LB film deposition, the dipping direction can be used to define the alignment direction of some second order NLO chromophores (8).

Organic Molecular Beam Deposition (OMBD)

In general, organic thin films can be deposited in solution or gas phase. Solution-based deposition is relatively easy to set up, and has been intensively studied. When we became involved in this field, we were, however, interested in an instrumentally sophisticated technique based on ultrahigh vacuum, referred to as organic molecular beam deposition (OMBD) (7). It is an offshoot of the physical vapor deposition (PVD) technique that has been widely used in microelectronic and optical industries for the deposition of inorganic thin films (9).

The OMBD process is illustrated in Figure 1. The materials in the effusion cells (d, Figure 1) are evaporated, and the gas molecules rush out of the small hole of the cell into the ultrahigh vacuum chamber, forming a molecular beam (f). Some of them stick on a relatively cold substrate (a) while the others are absorbed by the liquid nitrogen shroud (g). The ultrahigh vacuum (< 10^{-8} mbar) is generated by the turbo molecular pump (h) and the liquid nitrogen shroud (g). The film thickness can be monitored with monolayer sensitivity by the quartz thickness monitor (b) or the ellipsometer (c). The deposition (on/off) can be controlled by the shutters (e).

As compared to the solution-based growth techniques, OMBD has several practical advantages. It is carried out in ultrahigh vacuum that is an ultraclean environment. It enables precise and in-situ control of substrate temperature, growth rate, and film thickness. Because the molecules in the beam under ultrahigh vacuum are too far away to interact with each other, they fly straight. If the dimensions of the substrate are much shorter than the distance between the effusion cell and the substrate, the approaching direction of the gas molecules should be approximately the same over the whole film area. As discussed later, this unique “beam-like” feature can be used to align molecules in the film. From a practical point of view, it also allows easy fabrication of well defined and miniature patterns using masks in front of the substrate. In addition, OMBD can combine the deposition of metals, organics, and semiconductors in the same chamber with a predetermined sequence, composition, and layer thickness, for preparation of well defined hetero-layer structures. Moreover, high growth rates in the order of micrometers per hour are possible. Combining all these unique advantages, OMBD appeared to be an ideal tool for the fabrication of *e.g.* integrated optical and electrical circuits based on conjugated organic molecules.

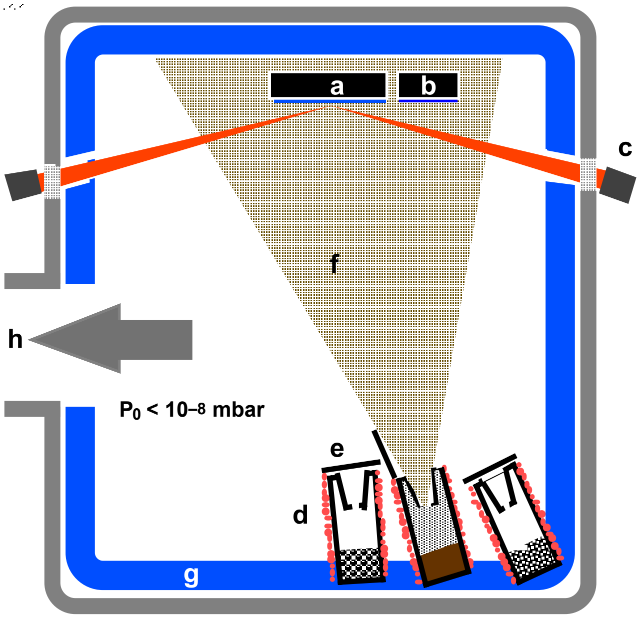

Figure 1. *Illustration of Organic Molecular Beam Deposition (OMBD). a: substrate; b: quartz crystal thickness monitor; c: ellipsometer; d: effusion cells; e: shutters; f: molecular beam; g: liquid nitrogen shroud; h: turbo molecular pump.*

Supramolecular Assemblies as Anisotropic Materials for OMBD

Despite the above advantages of OMBD, the technique has been far less developed for growth of anisotropic organic thin films as compared to the solution-based techniques. The main reason is probably that the OMBD technique is neither familiar nor accessible to many organic chemists. The shortage of input from organic chemistry hampers the development of materials for this technique.

Our main interest was to grow NLO thin films where the dipolar molecules are aligned in the same direction. In general, NLO materials can be grouped into two types: the low molecular weight crystalline materials and the polymers (1,2). It is extremely difficult to grow a large single crystalline film by OMBD. It has been demonstrated that an anisotropic polycrystalline film of 4'-nitrobenzylidene-3-acetamino-4-methoxy-aniline (MNBA), an efficient NLO material, can be grown on a centrosymmetric organic single crystal of ethylenediammonium terephthalate (10). Here, the anisotropy of the films is induced by the lattice-matched substrate surface (heteroepitaxy). However, it is difficult to apply this method to many practical inorganic substrates that are either amorphous or have a distinct lacttice constant from that of organic crystals. In fact, many well known low molecular weight NLO materials have been tried to grow on silicon and glass substrates, but at best resulting in films consisting of randomly oriented and µm-sized microcrystals that cause high scattering losses (11). On the other hand, polymers containing NLO chromophores can be easily processed to thin films by spin coating, and the dipolar chromophores can then be aligned by high electric field poling at the glass transition temperature of the polymer (1,2). Such films have a much better optical quality than the polycrystalline films of conventional low molecular weight materials. However, the non-volatile polymers are not suitable for OMBD, and the above mentioned unique advantages of OMBD are difficult to be realized with the polymer materials.

We reasoned that a compromise might be found by developing a new type of materials for OMBD based on supramolecular assemblies (12) where the molecules are linked to each other via strong and directional interactions such as hydrogen bonds (H-bonds). If the strong intermolecular bonds can be broken at elevated temperatures while the molecules are intact, then the materials might be suitable for OMBD. In addition, the grain boundary in such materials can be reduced (13) and the molecular alignment stabilized. Based on this idea, we designed a series of molecules having a pyridyl group at one end, and a carboxy group at the other, such as 4-[(pyridin-4-yl)vinyl]benzoic acid (**1**) and 4-[(pyridin-4-yl)ethynyl]benzoic acid (**2**) (Figure 2). They are expected to form strong and linear head-to-tail intermolecular H-bonds in the solid states (14-17).

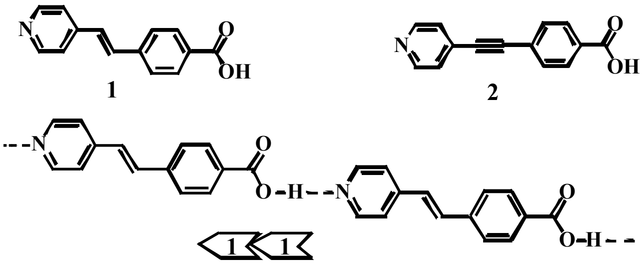

Figure 2*. Molecules that can form supramolecular assemblies in the solid states.*

Indeed, in the solid state ^{15}N-NMR spectra, the pyridyl ^{15}N signals of **1** and **2** appear at –105 and –106 ppm relative to that of $CH_3{}^{15}NO_2$ (0 ppm), while that of pyridine at –63 ppm, and that of the methyl ester of **2** at –67 ppm (15,16). The large upfield shift can only be attributed to the strong H-bonding to the pyridyl N-atom. Since there is only one peak found in the region of 0–200 ppm, it is unlikely that the solid state materials contain significant amount of short oligomers or dimers of the carboxylic acids. Otherwise, additional ^{15}N signals of the free pyridyl groups at the end of the oligomers and dimers should be present. In accord with the strong head-to-tail H-bonding, these low molecular weight materials have a high melting point (350°C for **1**, and 300°C for **2**), while the methyl ester of **1**, lacking intermolecular H-bonding, melts at 105–107°C. Compounds **1** and **2** can be sublimated at 250–220°C/0.01 mbar without decomposition, and thus are suitable for OMBD.

Self-Assembly of Nanostructures by OMBD

We reasoned that the superstructures of ultra-thin films of **1** and **2** on a flat metal surface might be observed directly by scanning tunneling microscopy (STM). A series of ultra-thin films of **1** were then grown on the Ag(111) surface by OMBD, and characterized by in situ STM (18). Since Ag is a noble metal, the absorbate/substrate interactions are weak, and in view of the smoothness of the close-packed (111) geometry, it was expected that the intermolecular interaction could be reflected by the molecular arrangement at the surface. Indeed, we found that upon deposition at 300 K **1** self-assembled into linear lines (the bright lines in Figure 3A) with a length of up to several µm and a width of only about 1 nm. The lines oriented along <112> directions of the Ag-lattice with mesoscopic ordering at the µm scale, only weakly affected by the atomic steps of the substrate surface. This corresponds to a one-dimensional nanograting, noting that the distance between the parallel lines was about 10 nm.

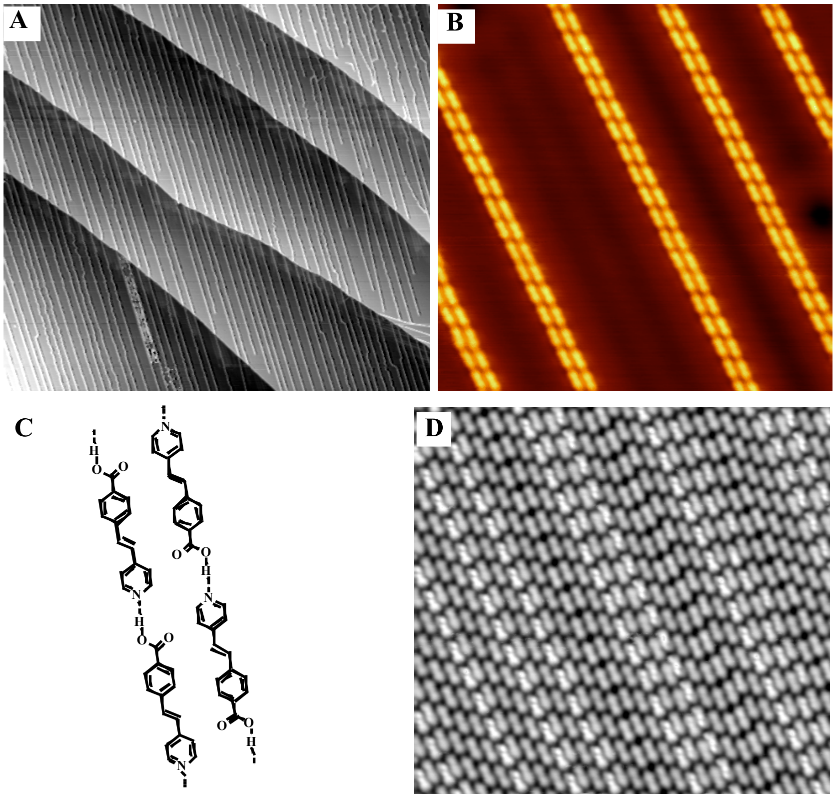

***Figure 3**. STM images of a submonolayer (A: 400 x 400 nm^2, B: 18 x 18 nm^2, C: model) and a monolayer (D, 20 x 20 nm^2) film of **1** grown on Ag(111) at 300K. Individual molecules of **1** are clearly resolved in the high resolution images B and D. The data were obtained at 77K. B is reproduced (permission pending) from ref. 18.*

As revealed by the high resolution STM image (Figure 3B), where individual molecules of **1** were clearly resolved, each line actually consisted of polymer twin chains of **1** hydrogen-bonded in a linear and head-to-tail fashion along the chain direction (18). An analysis of STM contours lines demonstrates that the molecules within the twin chains were oriented anti-parallel to each other, as illustrated in the corresponding model in Figure 3C (18). When the films were grown into monolayer coverage, the perfect one-dimensional ordering was retained as shown in Figure 3D.

Since the twin chains were anti-parallel to each other and the films consisted of three rotational (120°) domains due to the threefold symmetry of Ag(111), such films are centrosymmetric in the bulk form. Nevertheless, the results are highly interesting in relation to nanotechnology and molecular electronics (5). They demonstrate that supramolecular assemblies might be processed into molecular wires by OMBD.

Growth of Multi-Layer Films with an In-Plane Directional Order

For nonlinear optic applications, it is necessary to grow macroscopically ordered films with a thickness larger than tens of nanometers. Here the key problem is how to maintain the same degree of order over a large area and through increasing thickness. We have shown that **1** can self-assemble into long and linear supramolecular polymers in a head-to-tail fashion. But we needed to find a way to orient each polymer chain in the same direction.

Initially, we reasoned that if a substrate surface is functionalized so that it bonds only one end of the molecules **1** and **2**, the head-to-tail H-bonding of the continuously arriving molecules should lead to a molecular alignment in the direction that is perpendicular to the substrate surface (19). Following this idea, we silylated glass substrates with 2-(4-chlorosulfonylphenyl)ethyltrichlorosilane to provide a surface of sulfonic acid groups that prefer to bond the pyridyl group of *e.g.* **1** (Figure 4A). Films of **1** and **2** were then grown on the silylated and bare glass or quartz substrates for a comparison.

In our home-built OMBD chamber (Figure 1), the distance between the beam source and the substrate (2x2 cm^2) was 26 cm, hence the molecular beam direction over the whole substrate surface is almost constant (Figure 4B). The deposition angle, defined as the angle between the molecular beam and substrate surface normal, was ~26°. Before OMBD, **1** and **2** were ground into fine powder, and degassed at 100–120˚C/10^{-9} mbar overnight. The substrates were washed with acetone in ultrasound for 5 min, and then dried at 120ºC and 10^{-6} mbar for 0.5 h. During deposition, the base pressure was 5 x 10^{-9} mbar, the evaporation temperature was 230˚C, and the substrate temperature was varied between 30 and 100˚C. The deposition rate was about 5 nm/min. SHG experiments were performed using a BMI Nd:YAG laser at 1064 nm (7 ns pulses, 10 Hz repetition rate).

To our surprise, all experimental results (15-21) indicated that ***1** and **2** in the multilayer films were preferentially lying flat on the substrate surface. In addition, they had a preferential in-plane direction that was parallel (or antiparallel) to the X_3 axis, defined as the projection of molecular beam direction on the substrate surface* (Figure 4B). Moreover, the preferential molecular direction was the same over the *whole* large film area (2x2 cm^2), and was **not** dependent on the different types of glass substrates no matter whether they were functionalized or not (19). This means that the in-plane alignment direction can be chosen simply by rotating the substrate around the X_2 axis, because the alignment direction is only defined by the molecular beam direction. This conclusion was drawn from the following SHG experiments.

In the first experiment, the polarizations of the input and output laser beam were set parallel to the X_3 axis. We rotated the substrate around the X_1 axis and recorded the output second harmonic signal as a function of the laser incident angle, that is, the angle between the X_3 and the polarization axes. The result reproduced in Figure 4C (15) shows that the SHG signal reaches the maximum when the X_3 axis is parallel to the polarization. This indicates that the dominant second harmonic susceptibility tensor of the film is parallel to the substrate surface. According to our semiempirical calculations (AM1), the second-order polarizability of the linear assemblies of **1** and **2** is dominated by its tensor component along the long molecular axis. Therefore the results indicates that the molecules are lying flat on the surface.

To find out the in-plane alignment direction, we rotated the sample and recorded the second harmonic signal as a function of the angle between the X_3 and the polarization axes. As shown in Figure 4D (15), when the X_3 axis is parallel to the polarization axis, the SHG intensity reaches its maximum, and when X_3 is perpendicular to the polarization, it drops to zero. This indicates that the molecules are preferentially aligned along the X_3 axis.

The above results hold for films of **1** and **2** grown on silylated and bare glass, quartz, and indium tin oxide (ITO) substrates at substrate temperatures ranging from 30° to 100°C. In addition, the SHG intensities at different places of the films varied within 10% which was the experimental error, indicating the same degree of order over the whole large film area (2x2 cm^2). The most noteworthy result is that *the same degree of order was obtained with different thickness from 100 to at least 400 nm*, as shown by the quadratic relationship (22) of the SHG intensities with the film thickness (Figure 4D) (15). In contrast, we are not aware of any other self-assembled films that could maintain their initial order beyond a thickness of 100 nm. In general, the disorders tend to accumulate during the growth, although this problem might be overcome by the laborious and time consuming layer-by-layer methodology (4).

The films grown on glass below 100˚C were transparent and homogeneous. As revealed by scanning electron microscope (Figure 4E), films of **1** grown even at 100°C still had a featureless surface. The surface roughness (~ 5 nm) measured by atomic force microscopy was smaller than the roughness of the substrate surface. In contrast, the other low molecular weight NLO materials we examined readily formed µm-sized crystallites as observed by light microscope. The low tendency for **1** to form large crystallites can be attributed to the directional head-to-tail H-bonding which dominates the other intermolecular interactions. The strong H-bonding is also expected to stabilize the polar order. Indeed, the SHG intensity of the films decreased only slightly before reaching 190ºC for **1** and 180˚C for **2**.

Among the above results, the most intrigue one is that the molecular alignment direction is defined by the projection of the obliquely incident molecular beam on the substrate surface (X_3 axis). In fact, it took us a long time to come to this conclusion and to be convinced that the alignment was not due to the possible substrate anisotropy. But then how can we explain this? Imaging that the molecules in the molecular beam can rotate freely although they fly in the same direction, why should they preferentially align along the X_3 axis? In addition, why the same degree of order can be kept for hundreds of layers without accumulation of errors?

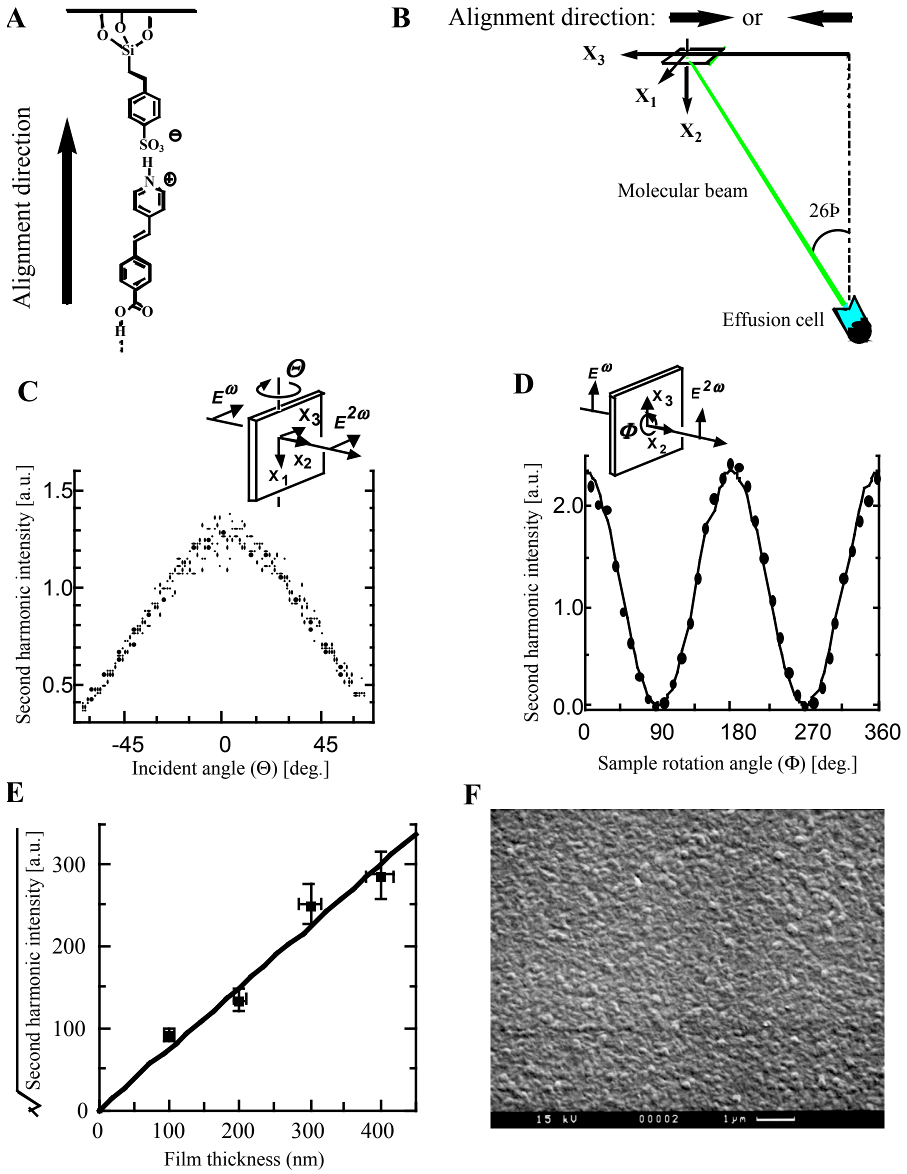

***Figure 4**. A: proposed alignment direction of **1** grown on silylated glass. B: setup for Oblique Incidence OMBD and the observed alignment direction of **1** and **2** on bare and silylated glass substrates. C: sample rotation angle dependent SHG. D: Incident angle dependent SHG. E. Thickness dependent SHG. F: SEM image of a film of **1** grown on glass at 100°C, reproduced from (15) (permission pending).*

Proposed Mechanism of Self-Assembly During OMBD

To answer the above questions, we need to consider details of the thin film growth process (17). First of all: why can the molecules in ultrahigh vacuum be deposited on a surface? Obviously, that is because the surface molecules bond the incoming molecules. This process can occur when the free energy of bonding is negative ($\Delta G = \Delta H - T\Delta S < 0$), that is, the enthalpy of bonding ($-\Delta H$) is larger than the entropy term ($-T\Delta S$) which favors dissociation particularly in ultrahigh vacuum. For **1** and **2**, the intermolecular interactions include H-bonding, van der Waas forces, and π-π stacking interaction. Without H-bonding, the other two bonding interactions appear too weak to keep the molecules from dissociating at room temperature. In fact, without a H-bond, the methyl ester of **1** has a dramatically lower melting point than **1** (106 vs 350°C). Materials with a melting point lower than 130°C usually cannot be deposited at 27°C by OMBD (11). The fact that films of **1** and **2** can be easily deposited even at 100°C should be due to the H-bonding.

Thermodynamic Aspects of the Hydrogen Bonding

For **1** and **2**, the strongest H-bonds are the tail-to-tail bonding and the head-to-tail bonding (Figure 5), and the former having two $OH^{\cdots}O$ bonds is stronger than the latter having only one $H^{\cdots}N$ bond. However, if many molecules are involved, the head-to-tail bonding that leads to supramolecular assemblies can be thermodynamically more favored, considering that each molecule in the chain has also two $H^{\cdots}N$ bonds (Figure 5) that should be stronger than the $H^{\cdots}O$ bonds. This is in accord with the above solid state ^{15}N-NMR studies that indicated the dominance of head-to-tail H-bonds. The enthalpy (ΔH) for dimerization of carboxylic acid derivatives is typically –15 kcal/mol, and the entropy (ΔS) is –36 cal/mol (23). Hence the dissociation temperature (when $\Delta G = 0$) for a tail-to-tail bond is 144°C. This is considerably higher than the desorption temperature of the film (128°C) measured by in situ ellipsometry (17). It suggests that the desorption may involves sequentially breaking the head-to-tail H-bonds of the surface molecules.

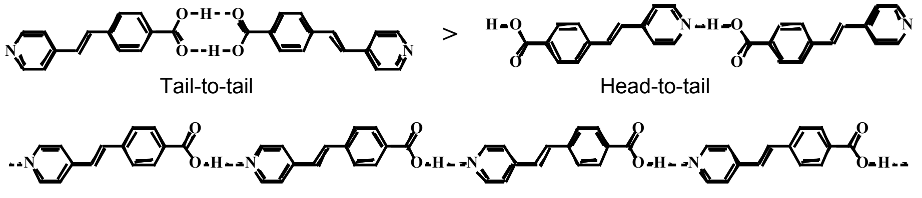

Tail-to-tail

Head-to-tail

***Figure 5**. The strongest H-bonds for **1**.*

Directional Requirement for Hydrogen Bonding

We have assumed that thin film growth of **1** and **2** is mainly due to the head-to-tail and tail-to-tail H-bonding. Now we need to consider the kinetics of the bonding. These bonds are most likely to form when two molecules collide in the ways shown by the large arrows in Figure 6, that is, the carboxy H-atom approaches another molecule along the axes of the non-bonding electron pairs at the O– or the N–atoms (24). If the collision happens in the other directions (the small arrow in Figure 6), the chance for the bonding is lower.

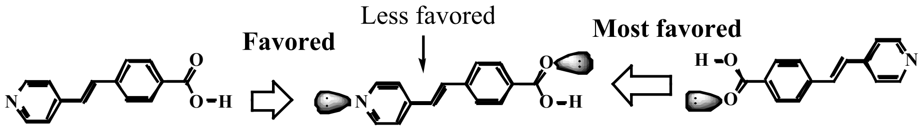

***Figure 6**. Illustration of the directional preference of H-bonding of **1**.*

As mentioned before, during OMBD, the molecules in the beam translate to the film surface in the same direction. *In this case, the H-bonding probability should be influenced by the orientation of the surface molecules.* This assumption was supported by the growth of **1** on Pd(110) surface at 27°C (25). Unlike Ag(111) surface, the Pd(110) surface bonds **1** strongly with an estimated bonding energy of ~65 kcal/mol (25). It forces **1** to lay flat on the Pd surface as shown by the in situ STM measurement (Figure 7). Interestingly, when the substrate surface was covered by a monolayer of **1** (Figure 7B) the growth stopped, that is, the incoming molecules could no longer bond to the already adsorbed molecules. This is probably due to the unfavorable orientations of the surface molecules that are determined by the substrate surface. This orientation provides the lowest chance for the surface molecules to hydrogen bond the incoming molecules (Figure 6), while the other intermolecular forces alone are too weak to keep additional molecules on the film surface. At low temperatures, those forces contribute more to the bonding of the arriving molecules, but they are far less directional than H-bonding, and the randomness is expected to increase. Indeed, the second harmonic intensity of the films of **1** grown at –190˚C was only about 10% of those grown at 30˚C (17).

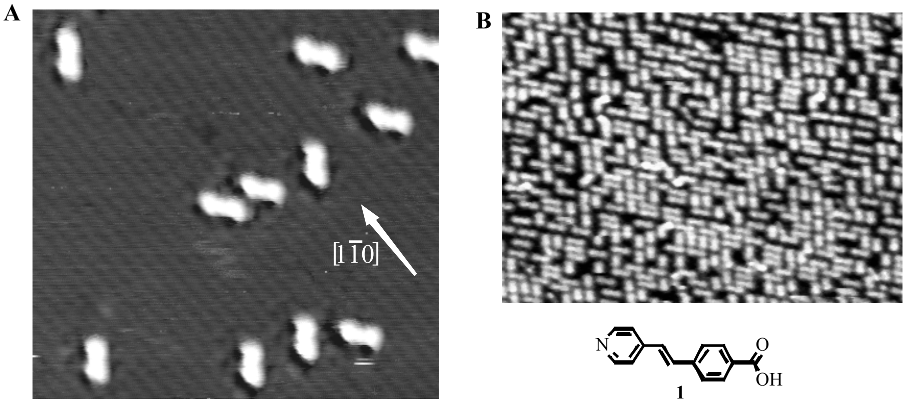

Figure 7. STM images of sub-monolayer(A) and monolayer(B) films of ***1*** *on Pd(110). Reproduced from (17) (permission pending).*

Self-Correcting Effect

So far, we arrive to the conclusion that the highest growth rate is obtained when the end group (the pyridyl or carboxy) of the surface molecules tilts towards the molecular beam direction. The following discussion gives a plausible answer to how it is possible to achieve a directional alignment that remains over hundreds of layers (17). When the first layer of the molecules are deposited on a glass substrate, both the pyridyl and carboxy groups can tilt towards the molecular beam direction to capture the arriving molecules (Figure 8). Because the pyridyl groups prefer to bond to the carboxy groups, after the bonding, the molecular direction will be preserved for the surface molecules with their pyridyl group facing to the incoming molecules (Figure 8, left). For those orienting their carboxy groups towards the incoming molecules, although head-to-tail bonding to the pyridyl groups of the arriving molecules is also possible, for both thermodynamic and kinetic reasons (Figure 6), they are more likely to capture the arriving molecules through the tail-to-tail bonding. Hence, after the bonding, more than half of the carboxy groups on the surface will be changed to the pyridyl groups (Figure 8, right). Accordingly, after growth of n layers, the ratio of pyridyl vs carboxy groups on the surface will be larger than $2^n/1$ (Figure 8). This mechanism allows **1** and **2** to "self-correct" errors occurring during the growth, and hence keep the same degree of order over hundreds of layers. It also explains why the same results were obtained for multi-layer films of **1** and **2** grown on different glass substrate surfaces. A similar example of this effect on polar inclusion compounds of channel-type hydrocarbon crystals and NLO guests was provided by Hulliger et al (26). However, why is the alignment direction in our case not parallel to the molecular beam direction but to its projection on the substrate surface? This can be rationalized by the self-shadowing effect (17).

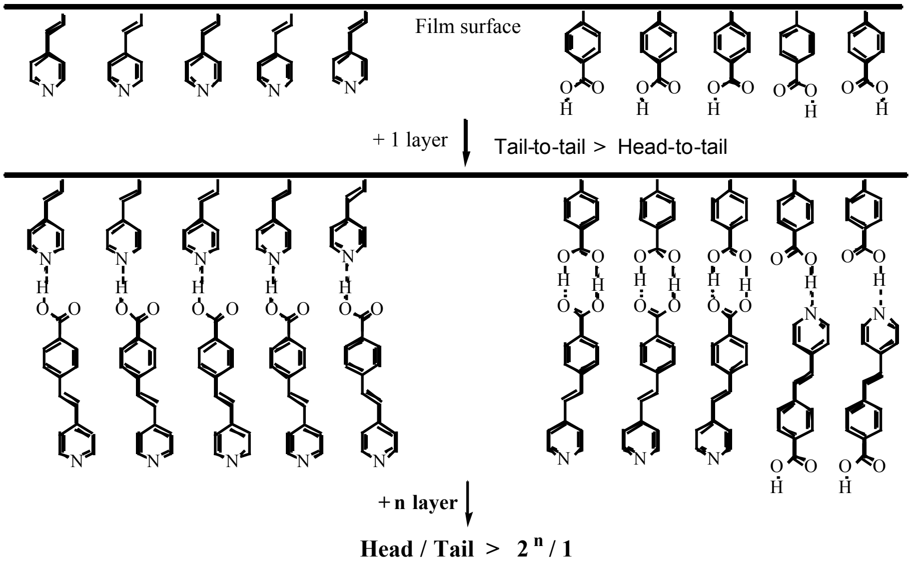

*Figure 8. Illustration of the "self-correcting effect" during OMBD with **1**.*

Self-Shadowing Effect

The self-shadowing effect is a kinetic phenomenum happening at non-equilibrium conditions (low substrate temperatures). When a molecule arrives at the film surface, it should choose the nearest and less crowded bonding site on the film surface. After bonding to the surface, it then blocks the subsequent molecules from reaching its shadowing area. This leads to void formation in the film. The effect is well known for oblique incidence molecular beam deposition of inorganic thin films. However, to our knowledge, it has not yet been reported for OMBD. Considering the large size of organic molecules, the shodowing effect should be more significant for OMBD. Formation of voids in the outmost layers during the growth of **1** is illustrated in Figure 9. The smallest void diameter should be larger than the molecular length. The highest surface density of the pyridyl groups and the optimal H-bonding geometry are provided to the arriving molecules only when the surface molecules and hence the voids are tilted towards the molecular beam direction. The sum of the weak van der Waals and π–π stacking interactions between the tilted chains increases with the chain length. These interactions attract the molecules to fill the voids for a close packing. The most probable way to fill the voids, while keeping the chain parallel to the molecular beam direction, is that the molecules in the inner layers lie in the X_3 direction on the substrate surface through a two-center hydrogen-bonded intermediate illustrated in the gray box in Figure 9. For voids along the X_1 axis, they can be filled through the migration of the tilted molecular chains along the X_1 axis (17).

Is the Orientation of the Arriving Molecules Random?

When the incoming molecules are far from the film surface, their orientation should be random. However, when they get close to the film, they start to feel the long range interactions from the film, especially the electro-static interaction. If the film is anisotropic, such interactions are expected to impose an orientation preference to the arriving molecules. This is more likely to happen in our system, where the films are not only anisotropic but also dipolar. The distance-dependent electro-static field as a sum over the molecules in the film appears to be quite large, although it remains to be calculated its significance relative to the rotational and translational kinetic energy of the arriving molecules which favors randomness. At first sight, the arriving molecules seemly prefer to orient anti-parallel to the surface molecules. However, it should be noted that **1** and **2** have a very different dipole moment when they are single molecules in the gas phase and when they are part of the supramolecular assemblies in the films. According to our AM1 calculations, the dipole moment of the arriving molecules is about 1 Debye. It mainly arises from the carboxy group and hence is perpendicular to the molecular axis as shown in Figure 9. For those molecules in the film, their dipole moment was calculated to be around 3 Debye and oriented along the molecular axis as illustrated by the upper large arrows in Figure 9. Therefore, the preferred orientation of the arriving molecules should be the one with the carboxy group facing to the film surface (Figure 9). That is the perfect orientation for H-bonding (Figure 6).

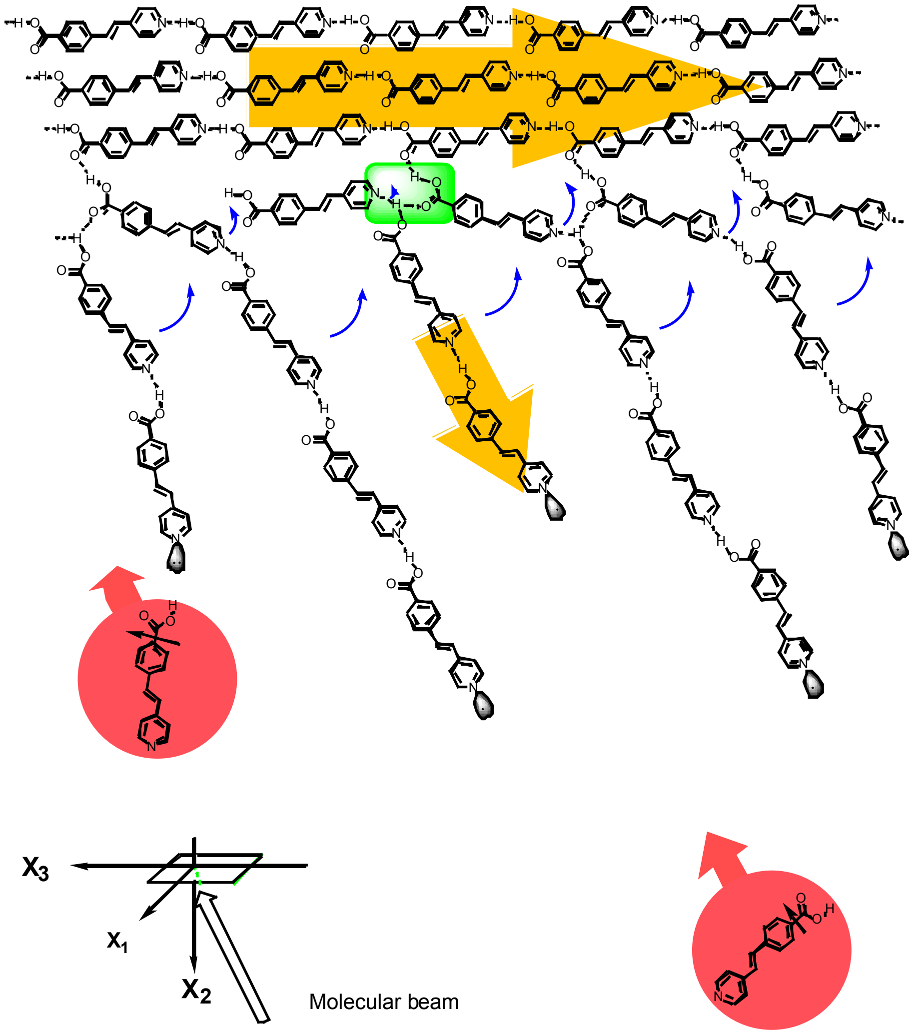

***Figure 9**. Proposed mechanism for alignment of **1** along the X_3 axis, the projection of the molecular beam direction on the film surface.*

Summary

OMBD has many technological advantages over solution-based methods for deposition of organic thin films and nanostructures. It calls for materials designed to take these advantages and to meet the requirements of specific applications. In this work, we present a new concept to grow anisotropic nanostructures and dipolar multi-layer thin films by OMBD. It began with a simple assumption that the use of rigid rod molecules such as **1** and **2** that can form strong and linear head-to-tail H-bonding may reduce randomness. The directional interaction dominates the other non-directional interactions, and thus an anisotropic order could be generated. This idea was supported by the formation of centrosymmetric anisotropic nanostructures consisting of supramolecular assemblies of **1**. Surprisingly, a macroscopic polar order can be generated in multi-layer films of **1** and **2** on amorphous glass substrates by oblique incidence OMBD. The polar order direction is parallel to the projection of the molecular beam direction on the substrate surface. This is remarkable for a molecular beam incident angle of only 30°. In addition, the films were grown out of one source rapidly and continuously. Moreover, the polar order was independent of the film thickness in the range of 100–400 nm. To account for these intriguing results, we proposed that the growth of **1** and **2** is mainly due to the H-bonding of the arriving molecules to the surface molecules. The bonding probability is determined by the orientation of the surface molecules relative to the well-defined approaching direction of the arriving molecules. Besides this effect, the self-correcting and self-shadowing effects that are associated with the shape and bonding features of **1** and **2**, as well as the long range directional interactions of the film with the arriving molecules, all are believed to contribute to the in-plane directional alignment of the molecules.

There are still several open questions. The nonlinear optical coefficients of the films are rather low, around 0.5–1 pm/V. This is expected for **1** and **2** which have a weak donor and acceptor. The degree of the ordering is still not clear, since the molecular nonlinearity cannot be measured. We are trying to address this question by synchrotron X-ray diffraction and scattering studies. The proposed mechanism also needs more quantitative theoretical support and further experimental verification.

Although the nonlinearities obtained with the prototype molecules are still too low for many practical applications, we have demonstrated that anisotropic films with a polar order can be obtained by oblique incidence OMBD with supramolecular assemblies based on strong and directional intermolecular interactions. Our results and proposed mechanisms are the first step in this topic which will be extended by improving the material design and processing conditions. The story also highlights the needs and opportunities for organic chemists to play an important role at the frontier of modern materials science and engineering.

References

1. Bosshard, C.; Sutter, K.; Prêtre, P.; Hulliger, J.; Flörsheimer, M.; Kaatz, P.; Günter, P. *Organic Nonlinear Optical Materials*, Gordon & Breach. Amsterdam, 1995.
2. *Organic Thin Films for Waveguiding Nonlinear Optics*; Kajzar, F.; Swalen J. D.; Eds.; Gordon & Breach: Amsterdam 1996.
3. Tredgold, R. H. *Order in Thin Organic Films*, Cambridge Univ. Press: Cambridge, 1994.
4. Ulman. A. *Chem. Rev.* **1996**, *96*, 1533–1554.

5. Reed, M. A. *Proceedings of the IEEE*, **1999**, *87*, 652.
6. Miyata, S.; Nalwa, H. S. Eds.; *Organic Electroluminescent Materials and Devices*, Gordon & Breach: Amsterdam, 1997.
7. Forrest, S. R. *Chem. Rev.* **1997**, *97*, 1793.
8. Decher, G.; Tieke, B.; Bosshard, C.; Günter, P. *Ferroelectrics* **1989**, *91*, 193.
9. Ohring, M. *The Materials Science of Thin Films*; Academic Press: Boston, 1992.
10. Dietrich, T.; Schlesser, R.; Erler, B.; Kündig, A.; Sitar, Z.; Günter, P. *J. Crystal Growth*, **1997**, *172*, 473.
11. Schlesser, R. Ph.D. Dissertation, ETH-Zürich, Switzerland, 1996.
12. Lehn, J.-M. *Supramolecular Chemistry,* VCH: Weinheim, 1995.
13. Sijbesma, R. P.; Beijer, F. H.; Brunsveld, L.; Folmer, B. J. B.; Hirschberg, J.; Lange, R. F. M.; Lowe, J. K. L.; Meijer, E. W. *Science*, **1997**, *278*, 1601.
14. The one-dimensional H-bond networks are shown in the crystal structure of isonicotinic acid, a lower analogue of **1** and **2**. Takusagawa, F.; Shimada, A. *Acta Crystallogr.* **1976**, *B32*, 1925.
15. Cai, C.; Bösch, M.; Tao, Y.; Müller, B.; Gan, Z.; Kündig, A.; Bosshard, C.; Liakatas, I.; Jäger, M.; Günter, P. *J. Am. Chem. Soc.* **1998**, *120*, 8563.
16. Cai, C.; Bösch, M.; Müller, B.; Tao, Y.; Kündig, A.; Bosshard, C.; Gan, Z.; Biaggio, I.; Liakatas, I.; Jäger, M.; Schwer, H.; Günter, P. *Adv. Mater.* **1999**, *11,* 745.
17. Cai, C.; Müller, B.; Weckesser, J.; Barth, J. V.; Tao, Y.; Bösch, M.; Kündig, A.; Bosshard, C.; Biaggio, I.; Günter, P. *Adv. Mater.* **1999**, *11,* 750.
18. Barth, J. V.; Weckesser, J.; Cai, C.; Günter, P.; Bürgi, L.; Jeandupeux, O.; Kern, K. *Angew. Chem.* Submitted.
19. Cai, C.; Bösch, M.; Tao, Y.; Müller, B.; Kündig, A.; Bosshard, C.; Günter, P. *Polymer Preprint*, **1998**, *39*(2), 1069.
20. Müller, B.; Cai, C.; Bösch, M.; Jäger, M.; Bosshard, C.; Günter, P.; Barth, J. V.; Weckesser, J.; Kern, K. *Thin Solid Films* **1999**, *343-344*, 171.
21. Müller, B.; Cai, C.; Kündig, A.; Tao, Y.; Bösch, M.; Jäger, M.; Bosshard, C.; Günter, P. *Appl. Phys. Lett.*, **1999**, *74*, 3110.
22. Lin, W.; Lin, W.; Wong, G. K.; Marks, T. J. *J. Am. Chem. Soc.* **1996**, *118*, 8034.
23. Curtiss, L. A.; Blander, M. *Chem. Rev*. **1988**, *88*, 827.
24. Legon, A. C.; Millen, D. J. *Acc. Chem. Res*. **1987**, *20*, 39.
25. Weckesser, J.; Barth, J. V.; Cai, C.; Müller, B.; Kern, K. *Surf. Sci*., **1999**, *431*, 168.
26. Roth, S. W.; Langley, P. J.; Quintel, A.; Wubbenhorst, M.; Rechsteiner, P.; Rogin, P.; Konig, O.; Hulliger, J. *Adv. Mater.* **1998**, *10*, 1543.